Analytica Chimica Acta 670 (2010) 51–56

Contents lists available at ScienceDirect

Analytica Chimica Acta

journal homepage: www.elsevier.com/locate/aca

Direct electrochemistry and electrocatalysis of horseradish peroxidase with hyaluronic acid–ionic liquid–cadmium sulfide nanorod composite material

Zhihong Zhu[a], Xia Li[b], Yan Wang[b], Yan Zeng[a], Wei Sun[b,*], Xintang Huang[a]

[a] Institute of Nano-Science and Technology Center, Huazhong Normal University, Wuhan 430079, PR China
[b] College of Chemistry and Molecular Engineering, Qingdao University of Science and Technology, Qingdao 266042, PR China

ARTICLE INFO

Article history:
Received 11 December 2009
Received in revised form 15 April 2010
Accepted 27 April 2010
Available online 6 May 2010

Keywords:
Hyaluronic acid
Horseradish peroxidase
Cadmium sulfide nanorod
1-Butyl-3-methylimidazolium tetrafluoroborate
Direct electrochemistry
Carbon ionic liquid electrode

ABSTRACT

A new composite material consisted of hyaluronic acid (HA), ionic liquid 1-butyl-3-methylimidazolium tetrafluoroborate ([BMIM]BF_4) and cadmium sulfide (CdS) nanorod was fabricated and used for the immobilization of horseradish peroxidase (HRP) on the surface of a carbon ionic liquid electrode (CILE), which was prepared with 1-ethyl-3-methyl-imidazolium ethylsulphate ([EMIM]$EtOSO_3$) as modifier. Spectroscopic results indicated that HRP remained its native structure in the composite film. Based on the synergistic effect of the materials used, an obvious promotion to the direct electron transfer efficient between HRP and CILE was achieved with a pair of well-defined redox peaks appeared in 0.1 mol L^{-1} phosphate buffer solution, indicating the realization of the direct electrochemistry of HRP. The immobilized HRP showed good electrocatalytic activity towards the reduction of trichloroacetic acid and H_2O_2 with the electrochemical parameters calculated. Based on the fabricated electrode, a new third-generation electrochemical biosensor was constructed with good stability and reproducibility.

1. Introduction

Direct electron transfer of metalloproteins with electrodes has aroused great interest in recent years due to the potential applications in the study of the redox properties of the biomolecules. The investigations can also provide useful information on the electron transfer mechanism and establish the foundation for the preparation of biosensors and bioreactors [1–4]. Different methods have been proposed to realize the direct electron transfer process. Among them the protein film modified electrodes have been widely studied because the presence of biocompatible film on the electrode surface can provide suitable microenvironments to keep the native structure of protein and accelerate the direct electron transfer rate between protein and electrodes [5,6]. Many composite films including biopolymers, sol–gel, nanomaterials and polyelectrolytes have been used in the film fabrication [7–14]. In recent years ionic liquids (ILs) have also been used for the fabrication of new kind of composite film. As a new type of green solvents with many specific properties such as high chemical stability, wide electrochemical windows and excellent ionic conductivity, ILs have exhibited potential applications in the field of electrochemical biosensors [15–18]. Wei and Ivaska reviewed the recent developments of ILs in electrochemical sensors [19]. ILs can be used as the supporting electrolyte or the modifier for chemically modified electrodes [20–22]. Wang et al. investigated the direct electrochemistry and electrocatalysis of heme proteins entrapped in agarose hydrogel films with IL as the electrolyte [23]. Ding et al. studied direct electrochemical response of myoglobin (Mb) on the plane graphite electrode with 1-(2-hydroxyethyl)-3-methyl imidazolium tetrafluoroborate as supporting electrolyte [24]. Sun et al. also applied IL modified carbon paste electrode for the investigation on the direct electrochemistry of hemoglobin (Hb) and Mb with different nanomaterials [25–27]. Liu et al. fabricated a carbon nanotubes-IL gel modified microelectrode and investigated its application in bioelectrochemistry [28].

Hyaluronic acid (HA) is a biodegradable, biocompatible, non-immunogenic and linear polysaccharide consisting of 2-acetamide-2-deoxy-α-D-glucose and β-D-glucuronic acid residues linked by alternate $(1\rightarrow3)$ and $(1\rightarrow4)$ glycoside bonding. As a weak polyelectrolyte with pK_a as 2.9, HA demonstrates a relatively low charge density even when all the carboxylic acid groups are ionized. HA has been widely used in biomedicine, tissue engineering, and drug delivery due to its good biocompatibility, nontoxicity and the formation of hydrogel membrane [29]. Recently, HA has also been used in the direct electrochemistry of proteins. Liu et al. adopted layer-by-layer method to assemble Mb and HA onto the basal-plane pyrolytic electrode and studied the electrochemical properties of Mb [30]. Gao et al. investigated the direct elec-

* Corresponding author. Tel.: +86 532 84022681; fax: +86 532 84023927.
E-mail address: sunwei@qust.edu.cn (W. Sun).

0003-2670/$ – see front matter © 2010 Elsevier B.V. All rights reserved.
doi:10.1016/j.aca.2010.04.061

trochemistry of Hb on the HA and 1-butyl-3-methylimidazolium tetrafluoroborate ([BMIM]BF_4) composite film modified electrode [31]. Ma et al. studied the direct electrochemistry and electrocatalysis of Hb by casting Hb–HA mixture on the edge-plane pyrolytic graphite electrode [32]. Cadmium sulfide (CdS) is a widely investigated semiconductor owing to its potential applications in the field of hydrogen production, solar cells, and photocatalysis. Various approaches, such as thermal evaporation, template method, aqueous solution and solvothermal process, have been applied to achieve CdS nanocrystals [33–35]. Due to the remarkable size dependent optical properties and interface effect, CdS nanomaterials exhibit the potential application in the bioelectrochemistry. Huang et al. applied CdS nanoparticle for the investigation on the direct electrochemistry of glucose oxidase (GOD) [36]. Wang et al. reported the detection of DNA hybridization with CdS nanoparticle tracers [37]. Zhou et al. immobilized Hb with CdS nanoparticles and investigated the electrochemical reactivity and peroxidase activity [38]. However to our knowledge no documents had been reported based on the HA–CdS nanorod-IL composite materials for protein electrochemistry.

In this paper a new bionanocomposite material was prepared by simply mixing HA, CdS nanorod and [BMIM]BF_4 together, which was further used for the immobilization of horseradish peroxidase (HRP). Direct electrochemistry of HRP in the composite material was realized with a pair of well-defined redox peaks appeared. The HRP modified electrode showed good electrocatalytic ability to the reduction of trichloroacetic acid (TCA) and H_2O_2 with wide linear range and good sensitivity.

2. Experimental

2.1. Reagents

1-Ethyl-3-methylimidazolium ethylsulphate ([EMIM]$EtOSO_3$) and 1-butyl-3-methyl-imidazolium tetrafluoroborate ([BMIM]BF_4) were purchased from Hangzhou Kemer Chemical Limited Company, China). Horseradish peroxidase (HRP, MW 40,000, Shanghai Kayon Biochemical Limited Company, China), hyaluronic acid (HA, Shangdong Linquhuayuan Limited Company, China), graphite powder (average particle size 30 μm, Shanghai Colloid Chemical Company, China), trichloroacetic acid (TCA, Tianjin Kemiou Chemical Limited Company, China) and hydrogen peroxide (H_2O_2, Yantai Sahe Chemical Limited Company, China) were used as received. CdS nanorods were prepared according to Ref. [35]. 0.1 mol L^{-1} phosphate buffer solutions (PBS) with various pH values were used as the supporting electrolyte. All the other chemicals used were of analytical reagent grade and doubly distilled water was used in all the experiments.

2.2. Apparatus

A CHI 750B electrochemical analyzer (Shanghai CH Instrument, China) was used for all the electrochemical measurements with a conventional three-electrode system consisted of a HRP modified electrode as working electrode, a platinum wire as auxiliary electrode and a saturated calomel electrode (SCE) as reference electrode. UV–Vis absorption and FT-IR spectra were recorded on Cary 50 probe spectrophotometer (Varian Company, Australia) and Tensor 27 FT-IR spectrophotometer (Bruker Company, Germany), respectively.

2.3. Preparation of the modified electrodes

IL modified carbon paste electrode (CILE) was prepared by mixing 0.20 mL of [EMIM]$EtOSO_3$, 0.80 mL of liquid paraffin and 3.2 g of graphite powder together in a mortar for 20 min. The carbon paste was packed firmly into a glass tube (Φ = 4 mm) and the electrical contact was established via a copper wire to the paste in the inner hole of the tube. The CILE surface was gently smoothed on a piece of weighing paper just before use.

HRP modified electrode was prepared with following procedure: 18 mg of HRP, 60 μL of [BMIM]BF_4, 250 μL of 4.0 mg mL^{-1} HA solution and 50 μL of 11.0 g L^{-1} CdS nanorod suspension solution were mixed together, diluted to 1.0 mL with 0.1 mol L^{-1} PBS (pH 7.0), and sonicated homogeneously. Then 8.0 μL of the mixture was cast onto the newly prepared CILE surface and left it to dry at room temperature. The resulted electrode was denoted as HA–HRP–CdS–IL/CILE. During the procedure a beaker was fitted tightly over the electrode so that the solvent could evaporate slowly and a uniform film could be formed on the electrode surface. Other modified electrodes including HA–HRP–CdS/CILE, HA–HRP–IL/CILE and HA–HRP/CILE, etc. were prepared by similar procedure and used for comparison. All the electrodes were stored at 4 °C when not in use.

2.4. Procedure

Electrochemical measurements were carried out in a 10 mL electrochemical cell containing 0.1 mol L^{-1} PBS, which was purged with highly purified nitrogen for 30 min before the experiments and maintained in a nitrogen atmosphere during the experiments. UV–Vis spectroscopic experiments were performed with a mixture solution of certain concentration of HA, HRP, CdS nanorod and [BMIM]BF_4 with doubly distilled water. The HA–HRP–CdS–IL film assembled on a glass slide was used for FT-IR measurements.

3. Results and discussion

3.1. Characteristic of the modified electrodes

Electrochemical impedance spectroscopy (EIS) is a valuable method to monitor the impedance changes of the electrode surface during the modification process. The semicircle diameter of Nyquist plot reflects the electron transfer resistance (R_{et}), which is resulted from the electron transfer of the redox probe $[Fe(CN)_6]^{3-/4-}$. Fig. 1(A) showed the EIS of different modified electrodes with the frequencies swept from 10^4 to 0.1 Hz. The R_{et} value of the CILE was got as 79.0 Ω (curve a), which was due to the presence of high ionic conductive IL in the carbon paste electrode. While the R_{et} of HA–HRP/CILE increased to 115.0 Ω (curve b), indicating the presence of HA and HRP on the electrode surface hindered the electron transfer. After adding IL or CdS nanorod in the HA–HRP composite materials, the R_{et} values of HA–HRP–IL/CILE and HA–HRP–CdS/CILE were estimated to be 99.1 Ω (curve c) and 83.4 Ω (curve d), respectively, which was smaller than that of HA–HRP/CILE. The results indicated the conductivity of the composite film was enhanced due to the presence of IL or CdS nanorod. The R_{et} value of HA–HRP–CdS–IL/CILE was further decreased to 60.2 Ω (curve e), indicating the synergistic effect of IL and CdS nanorod in the composite film contributed to the improvement of the conductivity of the composite film. Fig. 1(B) showed typical cyclic voltammograms of the modified electrodes in a $[Fe(CN)_6]^{3-/4-}$ solution. On the CILE a pair of well-defined redox peaks appeared (curve a) with the peak-to-peak separation (ΔE_p) as 0.135 V (vs. SCE). On the HA–HRP/CILE the redox peak current decreased with increase of the ΔE_p value (curve b), indicating the presence of HA–HRP film hindered the electron transfer rate of $[Fe(CN)_6]^{3-/4-}$. On the HA–HRP–IL/CILE the redox peak currents increased (curve c), which was due to the high ionic conductive IL present in the composite film. On the HA–HRP–CdS/CILE, the peak currents also increased (curve d), which was attributed to the CdS nanorod present in

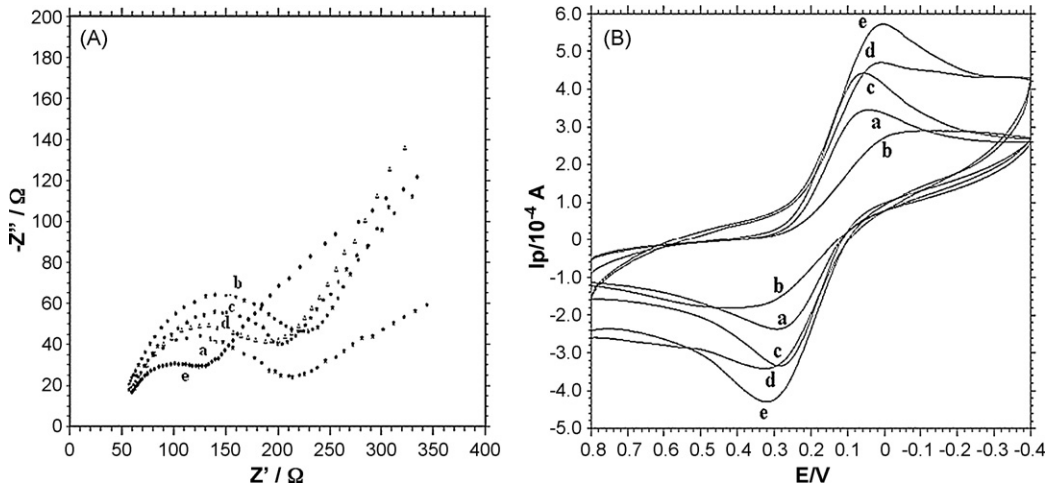

Fig. 1. (A) Electrochemical impedance spectroscopy for (a) bare CILE, (b) HA–HRP/CILE, (c) HA–HRP–IL/CILE, (d) HA–HRP–CdS/CILE and (e) HA–HRP–CdS–IL/CILE in the presence of 10.0 mmol L^{-1} $[Fe(CN)_6]^{3-/4-}$ and 0.1 mol L^{-1} KCl with the frequencies swept from 10^4 to 0.1 Hz; (B) cyclic voltammograms of (a) bare CILE, (b) HA–HRP/CILE, (c) HA–HRP–IL/CILE, (d) HA–HRP–CdS/CILE and (e) HA–HRP–CdS–IL/CILE in a mixture solution of 10.0 mmol L^{-1} $[Fe(CN)_6]^{3-/4-}$ and 0.1 mol L^{-1} KCl with scan rate as 100 mV s^{-1}.

the composite film. On the HA–HRP–CdS–IL/CILE, the redox peak current further increased (curve e) and was bigger than that of HA–HRP–CdS/CILE and HA–HRP–IL/CILE. The results also indicated the synergistic effect of CdS nanorod and IL in the composite film enhanced the electron transfer rate of the redox probe.

3.2. Spectroscopic results

UV–Vis absorption spectroscopy is a conventional method for monitoring the possible changes of the Soret band of heme proteins in the membrane modified electrode. The Soret band is sensitive to the variation of the microenvironment around the heme group and the band shift may provide the information about the denaturation in heme protein. Fig. 2(A) showed the UV–Vis spectra of HRP and its mixture with composite materials. Free HPR had a Soret band at 406.0 nm in water (curve a) and 409.0 nm in pH 3.0 PBS (curve b), indicating HRP was not denatured in pH 3.0 buffer solution. After HRP was mixed with the composite material, the Soret band appeared at 406.0 nm (curve c), indicating that HRP remained its native structure and no significant denaturation occurred to protein after mixed with the composite materials. The result showed the biocompatibility of the materials used in the composite film.

FT-IR spectroscopy is another sensitive method for the investigation on the secondary structure of proteins. The amide I and amide II band of protein can exhibit detailed information on the polypeptide chain. The amide I band at 1700–1600 cm^{-1} is attributed to the C=O stretching vibration of the peptide linkage in the backbone of protein. The amide II band at 1600–1500 cm^{-1} is caused by the combination of N–H inplane bending and C–N stretching vibration of the peptide groups [39]. If HRP molecule is denatured, the intensity and shape of the amide I and amide II bands will diminish or even disappear [40,41]. Fig. 2(B) showed the FT-IR spectra of HRP and its mixture with the composite material. Native HRP had the amide I and II band at 1657 and 1536 cm^{-1} (curve a), and the HRP in the composite film exhibited the similar positions at 1659 and 1572 cm^{-1} (curve b), indicating that the native structure of HRP was retained after mixed with the composite material.

Since IL is biocompatible green solvent with the ability to remain the native structure of enzyme. CdS nanorod has been proved to be a biocompatible nanomaterial and HA is a commonly used biocompatible film forming material in electrochemical biosensors. There is no doubt that HRP still maintain its biological structure in the composite film.

3.3. Cyclic voltammetric studies

Cyclic voltammograms of different modified electrodes in pH 3.0 PBS were shown in Fig. 3. In the case of HA–HRP/CILE, a pair

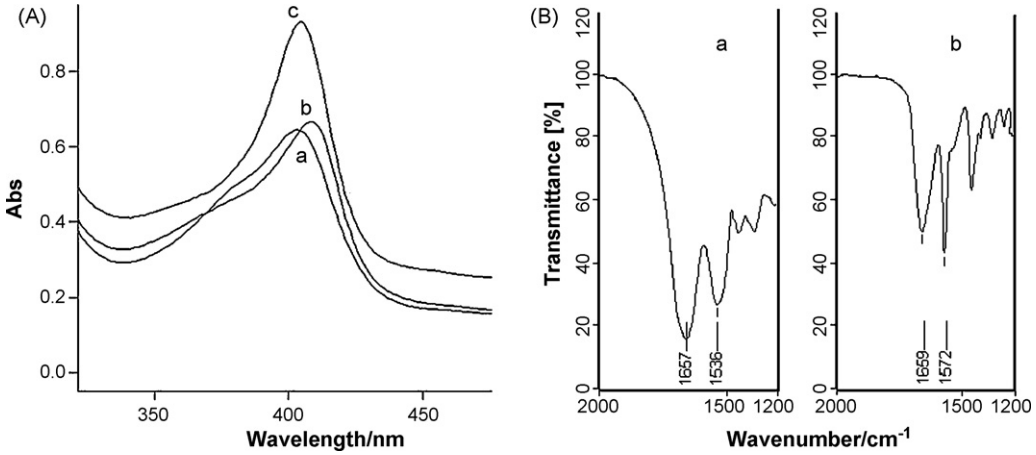

Fig. 2. (A) UV–Vis absorption spectra of (a) HRP in water, (b) HRP in pH 3.0 PBS and (c) HA–HRP–CdS–IL in pH 3.0 PBS; (B) FT-IR spectra of (a) HRP and (b) HA–HRP–CdS–IL film.

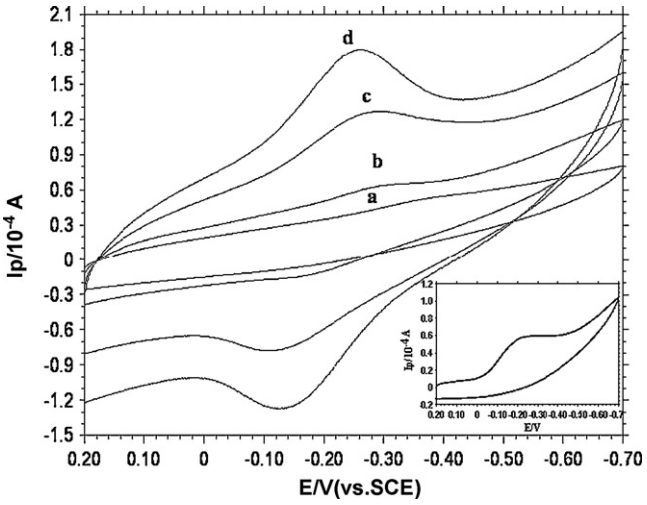

Fig. 3. Cyclic voltammograms of (a) HA–HRP/CILE, (b) HA–HRP-CdS/CILE, (c) HA–HRP–IL/CILE, (d) HA–HRP–CdS–IL/CILE and HA–HRP–CdS–IL/CPE (inset) in pH 3.0 PBS with scan rate as 100 mV s^{-1}.

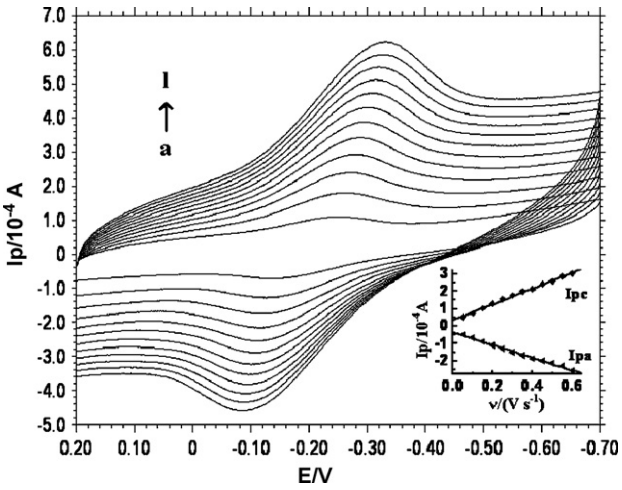

Fig. 4. Cyclic voltammograms of HA–HRP–CdS–IL/CILE in pH 3.0 PBS with the scan rates as 50, 100, 150, 200, 250, 300, 350, 400, 450, 500, 550 and 600 mV s^{-1} (from a to l), respectively. Inset: Linear relationship of anodic and cathodic peak current (I_p) versus scan rate.

of small redox peaks appeared with the oxidation and reduction peak potentials as −0.230 V (E_{pa}) and −0.363 V (E_{pc}), respectively (curve a). After CdS nanorod was added in the HA matrix, the redox peak current increased little than that of the HA–HRP/CILE (curve b), indicating the presence of CdS nanorod had some effect to facilitate the electron transfer rate. While on HA–HRP–IL/CILE (curve c) the redox peak current increased greatly with the redox peak potentials as −0.134 V (E_{pa}) and −0.266 V (E_{pc}). The results indicated that the addition of IL can greatly improve the electron transfer rate of HRP, which maybe contribute to the higher ionic conductivity of IL. The addition of IL in HA film can greatly increase the conductivity of the composite film. Cyclic voltammograms of HA–HRP-CdS–IL/CILE showed a further increase of the redox peak currents (curve d), which was bigger than the summary value of that of HA–CdS–HRP/CILE and HA–HRP–IL/CILE. The results indicated the synergistic augmentation of CdS nanorod and IL greatly promoted the electron transfer rate of HRP with the underlying electrode. The HA–CdS–IL nanocomposite material provided a biocompatible three-dimensional microenvironment for HRP to keep its native structure and remain its bioelectrochemical activity. For comparison the same nanocomposite material was applied on the surface of traditional CPE and cyclic voltammetric results indicated only a small reduction peak appeared (inset of Fig. 3). The result also proved the superiority of CILE to CPE. As indicated in Ref. [42], CILE can provide better reversibility and higher sensitivity than the traditional carbon electrode due to the presence of IL in the carbon paste.

From curve d the values of E_{pc} and E_{pa} were got as −0.248 and −0.139 V. The apparent formal potential ($E^{0'}$), which is calculated from the midpoint of the redox peak potentials, was got as −0.194 V (vs. SCE). The result was in accordance with the typical characteristic of HRP heme Fe(III)/Fe(II) redox couples [43]. The peak-to-peak separation (ΔE_p) was got as 0.109 V and the ratio of redox peak current was nearly a unity, which indicated a quasi-reversible process.

The influence of scan rate on the cyclic voltammetric response of HA–HRP–CdS–IL/CILE was further recorded with the results shown in Fig. 4. It can be seen that well-defined and symmetric redox peaks appeared in the scan rate range from 50 to 600 mV s^{-1}. Both the redox peak currents increased with the scan rate, and two linear regression equations were further calculated as I_{pa} (μA) = 0.351υ (V s^{-1}) + 4.52 (γ = 0.998) and I_{pc} (μA) = −0.345υ (V s^{-1}) − 3.66 (γ = 0.998), indicating a typical surface-controlled electrochemical process. With the increase of scan rate the peak-to-peak separation (ΔE_p) also increased gradually, so the electrochemical parameters of the electrode reaction were calculated according to the Laviron's equations [44]:

$$E_{pc} = E^{0'} - \frac{RT}{\alpha nF} \ln \upsilon$$

$$E_{pa} = E^{0'} + \frac{RT}{(1-\alpha)nF} \ln \upsilon$$

$$\log k_s = \alpha \log(1-\alpha) + (1-\alpha)\log\alpha - \log\left(\frac{2.3RT}{nF\upsilon}\right) - \alpha(1-\alpha)\frac{nF\Delta E_p}{2.3RT}$$

where α is the charge transfer coefficient, n is the number of electrons transferred and k_s is the apparent heterogeneous electron transfer rate constant. Two straight lines were got with the equations as E_{pa} (V) = 0.331 ln ν − 0.0323 (γ = 0.997) and E_{pc} (V) = −0.0974 ln ν + 0.022 (γ = 0.992). Then the values of α and k_s were calculated as 0.405 and 0.655 s^{-1}, respectively. The integration of the reduction peaks gave nearly the constant charge value (Q) at different scan rates. By integration the cyclic voltammetric curve and based on the Faraday's equation of $\Gamma^* = Q/nAF$, the surface concentration (Γ^*) of electroactive HRP on the modified electrode was calculated as 1.74×10^{-9} mol cm^{-2}. The value is two orders of magnitude higher than that of HRP in DNA modified pyrolytic graphite electrode (PGE) (5.10×10^{-11} mol cm^{-2}) [45], Eastman AQ modified PGE (9.10×10^{-11} mol cm^{-2}) [46], or clay–chitosan (CTS)-gold nanoparticle nanocomposite modified glassy carbon electrode (GCE) (2.1×10^{-11} mol cm^{-2}) [47], indicating that multilayers of HRP in the composite film take part in the electrode reaction. The result was attributed to the high surface area of CdS nanorod and excellent conductivity of the HA–IL composite materials. While the total amount of HRP immobilized on the electrode surface was 2.87×10^{-6} mol cm^{-2}, so 19.2% of the HRP molecules on the electrode surface took part in the electrochemical reaction, which is also larger than that of HRP-CTS film modified PGE (0.2%) or HRP-CTS-[Bmim][BF_4] (1-butyl-3-methylimidazolium tetrafluoroborate) film modified GCE (0.47%) [48,49]. The results demonstrated that the composite film provided a three-dimensional network for multilayers of HRP to exchange the electron with the electrode.

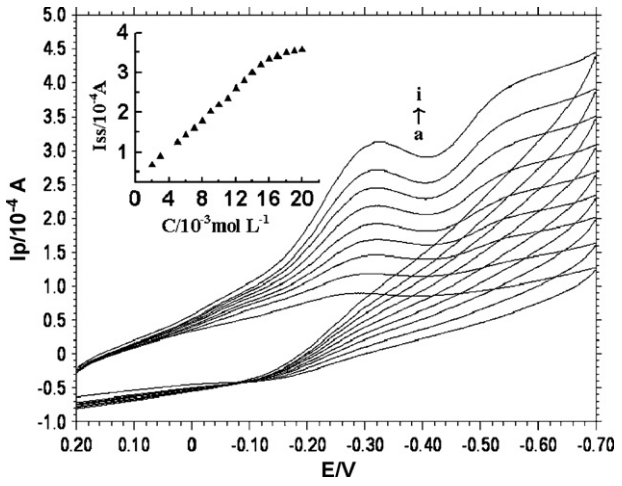

Fig. 5. Cyclic voltammograms of HA–HRP–CdS–IL/CILE in 0.1 mol L^{-1} pH 3.0 PBS containing 0, 1.6, 2.0, 6.0, 8.0, 10.0, 12.0, 14.0 and 18.0 mmol L^{-1} TCA (curve a–i), respectively, with the scan rate as 100 mV s^{-1}. Inset: Relationship of catalytic reduction peak currents with the TCA concentration.

3.4. Electrocatalysis

The HA–HRP–CdS–IL/CILE showed good electrocatalytic ability to the reduction of different substrates such as TCA and H_2O_2. Fig. 5 showed the cyclic voltammograms of the HRP modified electrode in 0.1 mol L^{-1} PBS containing different amounts of TCA. With the increase of TCA concentration a significant increase of the reduction peak current was observed with the disappearance of the oxidation peak, demonstrating a typical electrocatalytic reduction reaction. Based on the references [50,51] the electrocatalytic mechanism is proposed as follows:

$$\text{HRPFe(III)} + e \rightarrow \text{HRPFe(II)}$$

$$2\text{HRPFe(II)} + Cl_3CCOOH + H^+ \rightarrow 2\text{HRPFe(III)} + Cl_2CHCOOH + Cl^-$$

The catalytic reduction peak currents increased with the TCA concentration in the range from 1.6 to 18.0 mmol L^{-1} with the linear regression equation as I_{pc} (μA) = 0.262C (mmol L^{-1}) + 0.195 (γ = 0.999) and the detection limit as 0.53 mmol L^{-1} (3σ). The detection limit was smaller than that of Nafion-CdS-Hb modified CILE (10.0 mmol L^{-1}) [52] and {poly-diallyldimethylammonium/Hb}$_8$ films modified PGE (1.98 mmol L^{-1}) [53]. When the TCA concentration was more than 18.0 mmol L^{-1}, the peak current leveled off to a plateau, indicating a typical Michaelis–Menten kinetic mechanism. So the apparent Michaelis–Menten constant (K_M^{app}) was further calculated from the electrochemical version of Lineweaver–Burk equation [54] to evaluate the catalytic activity of the immobilized HRP. Based on the equation of $1/I_{ss} = (1/I_{max})(1 + K_M^{app}/C)$, where I_{ss} is the steady current after the addition of substrate, C is the bulk concentration of the substrate, and I_{max} is the maximum current measured under saturated substrate condition. The value of K_M^{app} was calculated as 0.345 mmol L^{-1}, which was smaller than that of HRP immobilized in agarose hydrogel films in [Bmim][PF_6] (1-butyl-3-methylimidazolium hexafluorophosphate) on GCE (52 mmol L^{-1}) [55] and Nafion-nano-$CaCO_3$-Hb film modified CILE (2.57 mmol L^{-1}) [25], suggesting a high affinity of HRP to TCA.

The HA–HRP–CdS–IL/CILE also showed good electrocatalytic ability to the reduction of H_2O_2. With the addition of H_2O_2 into pH 3.0 PBS the reduction peak current was also greatly enhanced corresponding with the decrease of the oxidation peak current. The more the H_2O_2 added, the larger the reduction peak current got, which indicated that HRP immobilized in the composite film could act as an effective catalyst to the reduction of H_2O_2. The mechanism of catalytic reduction of the immobilized HRP to H_2O_2 is exemplified by the following schemes [56]:

$$\text{HRP}(Fe^{3+}) + H_2O_2 \rightarrow \text{CompoundI}(Fe^{4+}{=}O) + H_2O$$

$$\text{CompoundI}(Fe^{4+}{=}O) + H^+ + e \rightarrow \text{CompoundII}$$

$$\text{CompoundII} + H^+ + e \rightarrow \text{HRP}(Fe^{3+}) + H_2O$$

The catalytic peak current changed linearly with H_2O_2 concentration in the range from 10.0 to 170.0 μmol L^{-1} with the linear regression equation as I_{pc} (μA) = 5.046C (mmol L^{-1}) + 18.21 (γ = 0.999) and the detection limit as 3.30 μmol L^{-1} (3σ). The detection limit is much smaller than those obtained from HRP in the clay-CTS-gold nanoparticle nanocomposite modified GCE (9.0 μmol L^{-1}) [47] and HRP in the sol–gel-derived ceramic–carbon nanotube modified GCE (12.89 μmol L^{-1}) [57]. When the concentration of H_2O_2 was more than 170.0 μmol L^{-1}, a plateau of peak current appeared, indicating a typical Michaelis–Menten kinetic process. So the apparent Michaelis–Menten constant (K_M^{app}) was further calculated from the electrochemical version of Lineweaver–Burk equation with the result as 0.012 mmol L^{-1}. The value is much smaller than those obtained from CdS-Hb modified PEG (3.48 mmol L^{-1}) [38], the sol–gel CPE (4.8 mmol L^{-1}) [58], and HRP immobilized in porous titania sol–gel modified GCE (1.89 ± 0.21 mmol L^{-1}) [59].

3.5. Stability and reproducibility

The HA–HRP–CdS–IL/CILE was continuous scanned in pH 3.0 PBS for 50 cycles and no decrease of the voltammetric response appeared, indicating the higher stability of the modified electrode in buffer solution. The HRP modified electrode was stored at 4 °C when not in use and 95.6% of the initial current response was retained after 2 weeks storage. After 1 month storage, the peak current response decreased about 9.5%. The good stability of the HRP electrode can be attributed to the biocompatibility of the HA–CdS–IL composite film, which can retain the secondary structure of the protein. Six HRP modified electrodes were prepared by the same procedure independently and the relative standard deviation (RSD) for the determination of 6.0 mmol L^{-1} TCA was calculated as 3.6%, which indicated the modified electrode had good repeatability.

3.6. Analytical application

The fabricated electrode was applied to detect the H_2O_2 concentration in the real sample of disinfector, which was produced

Table 1
Detection results of H_2O_2 in disinfector sample (n = 3).

Sample	Detected (mM)	Added (mM)	Found (mM)	Recovery (%)	RSD (%)
1	0.431	0.40	0.405	101.25	2.98
2	0.444	0.80	0.836	104.5	1.87
3	0.439	1.00	0.987	98.7	3.50

by Shandong Lircon Disinfection Technology Co., Ltd. Under the selected conditions and by using the standard addition method, the determination results were summarized in Table 1. It can be seen that the results were satisfactory with the recoveries in the range of 98.7–104.5%.

4. Conclusion

In this paper a new organic-inorganic hybrid nanocomposite material composed of CdS nanorod, HA and ionic liquid [BMIM]BF_4 was fabricated and further applied to immobilize HRP on the surface of CILE to get a new kind of electrochemical HRP biosensor. The formed composite material is biocompatible and integrates the advantages of the substances used, including the high conductivity of IL, the biocompatiblity and film forming ability of HA and the specific characteristics of CdS nanorod. Spectroscopic results indicated that the immobilized HRP still remained its native structure in the composite film. Direct electron transfer between HRP with the underlying electrode was realized with a pair of well-defined redox peaks appeared. The combination of CdS nanorod, ionic liquid and HA provided a suitable microenvironment for HRP to retain its native structure and biological activity. The electrochemical behaviors of HRP in the modified electrode were carefully investigated with the electrochemical parameters calculated. The HA–HRP–CdS–IL/CILE showed good electrocatalytic ability to the electrochemical reduction of TCA and H_2O_2, which provided a stable platform for developing a new kind of third-generation biosensor.

Acknowledgements

We are grateful to the financial support of the National Science Foundation of China (No. 50802032), Young Scientist Chenguang Project of Wuhan and Shandong Province Natural Science Foundation (ZR2009BL017).

References

[1] Y. Xiao, H.X. Ju, H.Y. Chen, Anal. Biochem. 278 (2000) 22–28.
[2] H.Y. Gu, A.M. Yu, H.Y. Chen, J. Electroanal. Chem. 516 (2001) 119–126.
[3] V.V. Shumyantseva, Y.D. Ivanov, N. Bistolas, F.W. Scheller, A.I. Archakov, U. Wollenberger, Anal. Chem. 76 (2004) 6046–6052.
[4] W.J. Zhang, G.X. Li, Anal. Sci. 20 (2004) 603–609.
[5] Z.H. Dai, H.X. Ju, H.Y. Chen, Electroanalysis 17 (2005) 862–868.
[6] F. Zhao, X. Wu, M.K. Wang, Y. Liu, L.X. Gao, S.J. Dong, Anal. Chem. 76 (2004) 4960–4967.
[7] H. Sun, H.Y. Ma, N.F. Hu, Bioelectrochem. Bioenerg. 49 (1999) 1–10.
[8] Q.L. Wang, G.X. Lu, B. Yang, Langmuir 20 (2004) 1342–1347.
[9] L.D. Zhu, C.A. Tian, J.L. Zhai, R.L. Yang, Sens. Actuators B: Chem. 125 (2007) 254–261.
[10] H.Y. Liu, N.F. Hu, Anal. Chim. Acta 481 (2003) 91–99.
[11] E. Topoglidis, C.J. Campbell, A.E.G. Cass, Langmuir 17 (2001) 7899–7906.
[12] X.J. Liu, Y.X. Huang, L.B. Shang, X.Y. Wang, H. Xiao, G.X. Li, Bioelectrochemistry 68 (2006) 98–104.
[13] C.Y. Liu, J.M. Hu, Biosens. Bioelectron 24 (2009) 2149–2154.
[14] X.L. Zhu, I. Yuri, X. Gan, I. Suzuki, G.X. Li, Biosens. Bioelectron 22 (2007) 1600–1604.
[15] M.C. Buzzeo, R.G. Evans, R.G. Compton, ChemPhysChem 5 (2004) 1106–1120.
[16] N. Maleki, A. Safavi, F. Sedaghati, F. Tajabadi, Anal. Biochem. 369 (2007) 149–153.
[17] M. Musameh, J. Wang, Anal. Chim. Acta 606 (2008) 45–49.
[18] J.L. Anderson, D.W. Armstrong, G.T. Wei, Anal. Chem. 78 (2006) 2892–2902.
[19] D. Wei, A. Ivaska, Anal. Chim. Acta 607 (2008) 126–135.
[20] N. Maleki, A. Safavi, F. Tajabadi, Anal. Chem. 78 (2006) 3820–3826.
[21] X.B. Lu, J.Q. Hu, X. Yao, Z.P. Wang, J.H. Li, Biomacromolecules 7 (2006) 975–980.
[22] P. Yu, Y.Q. Lin, L. Xiang, Langmuir 21 (2005) 9000–9006.
[23] S.F. Wang, T. Chen, Z.L. Zhang, D.W. Pang, K.Y. Wong, Electrochem. Commun. 9 (2007) 1709–1714.
[24] S.F. Ding, M.Q. Xu, G.C. Zhao, X.W. Wei, Electrochem. Commun. 9 (2007) 216–220.
[25] W. Sun, R.F. Gao, K. Jiao, J. Phys. Chem. B 111 (2007) 4560–4567.
[26] W. Sun, Z.Q. Zhai, D.D. Wang, S.F. Liu, K. Jiao, Bioelectrochemistry 74 (2009) 295–300.
[27] W. Sun, X.Q. Li, P. Qin, K. Jiao, J. Phys. Chem. C 113 (2009) 11294–11300.
[28] Y. Liu, X.Q. Zou, S.J. Dong, Electrochem. Commun. 8 (2006) 1429–1434.
[29] Y. Zhang, J.B. Zheng, Electrochem. Commun. 10 (2008) 1400–1403.
[30] H.Y. Liu, N.F. Hu, J. Phys. Chem. B 110 (2006) 14494–14502.
[31] R.F. Gao, X.D. Shangguan, G.J. Qiao, J.B. Zheng, Electroanalysis 20 (2008) 2537–2542.
[32] L. Ma, Y.N. Tian, Z.J. Rong, J. Biochem. Biophys. Methods 70 (2007) 657–662.
[33] M. Chen, Y. Xie, J. Liu, Y. Xiong, S. Zhang, Y. Qian, X. Liu, J. Mater. Chem. 12 (2002) 748–753.
[34] G. Shen, J.H. Cho, J.K. Yoo, G.C. Yi, C.L. Lee, J. Phys. Chem. B 109 (2005) 5491–5496.
[35] F. Wei, G.C. Li, Z.K. Zhang, J. Nanopart. Res. 7 (2005) 685–689.
[36] Y.X. Huang, W.J. Zhang, H. Xiao, G.X. Li, Biosens. Bioelectron 21 (2005) 817–821.
[37] J. Wang, G.D. Liu, R. Polsky, A. Merkoci, Electrochem. Commun. 4 (2005) 722–726.
[38] H. Zhou, X. Gan, T. Liu, Q.L. Yang, G.X. Li, J. Biochem. Biophys. Methods 64 (2005) 38–45.
[39] J.K. Kauppinen, D.J. Moffatt, H.H. Mantsch, D.G. Cameron, Appl. Spectrosc. 35 (1981) 271–276.
[40] Y.P. Song, M.C. Petty, J. Yarwood, W.J. Feast, J. Tsibouklis, S. Mukherjee, Langmuir 8 (1992) 257–261.
[41] A.E. Nassar, W.S. Willis, J.F. Rusling, Anal. Chem. 67 (1995) 2386–2392.
[42] H.T. Liu, P. He, Z.Y. Li, C.Y. Sun, L.H. Shi, Y. Liu, G.Y. Zhu, J.H. Li, Electrochem. Commun. 7 (2005) 1357–1363.
[43] G.Z. Liu, J.J. Gooding, Langmuir 22 (2006) 7421–7430.
[44] E. Laviron, J. Electroanal. Chem. 101 (1979) 19–28.
[45] X. Chen, C. Ruan, J. Kong, J. Deng, Anal. Chim. Acta 412 (2000) 89–98.
[46] R. Huang, N.F. Hu, Bioelectrochemistry 54 (2001) 75–81.
[47] X.J. Zhao, Z.B. Mai, X.H. Kang, X.Y. Zou, Biosens. Bioelectron 23 (2008) 1032–1038.
[48] H. Huang, N. Hu, Y. Zeng, G. Zhou, Anal. Biochem. 308 (2002) 141–151.
[49] J.S. Long, D.S. Silvester, G.G. Wildgoose, A.E. Surkus, G.U. Flechsig, R.G. Compton, Bioelectrochemistry 74 (2008) 183–187.
[50] X.S. Yang, X. Chen, X. Zhang, W.S. Yang, D.G. Evans, Sens. Actuators B: Chem. 134 (2008) 182–188.
[51] W. Sun, X.Q. Li, K. Jiao, Electroanalysis 21 (2009) 959–964.
[52] W. Sun, D.D. Wang, G.C. Li, Z.Q. Zhai, R.J. Zhao, K. Jiao, Electrochim. Acta 53 (2008) 8217–8221.
[53] P.L. He, N.F. Hu, G. Zhou, Biomacromolecules 3 (2002) 139–146.
[54] R.A. Kamin, G.S. Wilson, Anal. Chem. 52 (1980) 1198–1205.
[55] S.F. Wang, T. Chen, Z.L. Zhang, X.C. Shen, Z.X. Lu, D.W. Pang, K.Y. Wong, Langmuir 21 (2005) 9260–9266.
[56] T. Ferri, A. Poscia, R. Santucci, Bioelectrochem. Bioenerg. 45 (1998) 221–226.
[57] H.J. Chen, S.J. Dong, Biosens. Bioelectron 22 (2007) 1811–1815.
[58] J. Li, S.N. Tan, H.L. Ge, Anal. Chim. Acta 335 (1996) 137–145.
[59] J.H. Yu, H.X. Ju, Anal. Chem. 74 (2002) 3579–3583.